A review of multi-physics approaches for imaging sub-basalt sediments

Lucy MacGregor*

Cognitive Geology Ltd.

**lucymacgregor@googlemail.com*

Abstract

The presence of high velocity layers, such as basalt, carbonate or salt, can make the detection and characterisation of sediments lying beneath using conventional seismic techniques a difficult task. In such situations complementary information derived from measurements of electrical resistivity can provide valuable additional constraints on the structure both of the basalt layers and of any sediments lying beneath. Such approaches are particularly powerful when combined with seismic data in multi-physics workflows, which make full use of the strengths of each technology.

Several electromagnetic techniques have been developed and applied in the hydrocarbon exploration industry in recent years to address the problem of mapping electrical resistivity structure. The controlled source electromagnetic (CSEM) method uses a horizontal electric dipole source to transmit a low frequency (from a few tenths to a few tens of Hz) electromagnetic signal to an array of receivers which detect and record the resulting electric and/or magnetic fields. By studying the variation in amplitude and phase of the received signal, the resistivity structure of the sub-surface can be determined.

The magnetotelluric (MT) method uses measurements of naturally occurring electromagnetic fields to determine the resistivity of the sub-surface. The depth to which the incident EM fields penetrate depends on the frequency of the field and the resistivity of the medium. Thus, by studying the variation in response as a function of frequency, the variation in resistivity as a function of depth may be determined. Typically, the resolution of the MT method (in particular to thin resistive structures) is lower than the CSEM method, however MT signals penetrate to greater depth in the earth.

Both CSEM and MT methods have found application in characterisation of basalt layers and the sediments beneath. In the case of relatively thin basalt layers, the CSEM method is the most applicable. For more massive basalt, and to understand the deeper structure, MT methods may be more appropriate. In both cases careful integration with complementary information from gravity, magnetics or seismic is critical. Structural information from seismic plays a particularly important role.

Introduction

There are many areas of the world where potentially prospective sediments are obscured by volcanic layers. Determining the presence, properties and structure of such sediments is important in planning exploration campaigns. Despite many recent advances in seismic acquisition, processing and imaging, this remains a challenging task.

In recent years the value of multi-physics approaches to such problems has been recognised. All geophysical methods have strengths and weaknesses and when considered in isolation often provide incomplete or ambiguous information. However, when different methods are combined, the strengths in one can compensate for the weaknesses in another, giving a more complete and better constrained result overall.

A good example of this is the determination of the properties of a reservoir in a rock physics driven reservoir characterisation workflow. Seismic information can be used to determine structure and stratigraphy, and rock physics driven inversion workflows can be used to determine properties such as porosity and lithology in the reservoir. However, when taken alone seismic often struggles to distinguish residual hydrocarbons, from commercial accumulations, a key parameter that must be understood when making drilling decisions. In this situation, electromagnetic technologies can be used to provide complementary resistivity information, which when carefully integrated with seismic results can resolve such ambiguities. Examples of this application are provided by Alvarez et al., 2017 and 2018.

The problem of imaging sub-basalt sediments considered here can also be addressed using a multi-physics approach. In this case, seismic data can be used to image the top of the basalt. However imaging beneath the basalt is extremely challenging because of the high velocity and extreme heterogeneity of the basalt layers. In order to assess the prospectivity beneath basalt layers it is important to understand firstly whether sediments exist at all and if they do whether they are within a depth range to accommodate hydrocarbons. In order to image such sediments it is important to build accurate velocity models to allow robust migration of seismic data. Multi-physics approaches use complementary information from electromagnetic or gravity surveys to support the interpretation of both the basalt and sub-basalt structure, leading to more complete seismic images, and a better overall understanding of the geology and prospectivity.

Electromagnetic technologies

Electromagnetic technologies provide a valuable complement to traditional seismic methods, both in reservoir characterisation workflows (for example, MacGregor, 2012a, b; Alvarez et al., 2017 and 2018) and in structural imaging problems such as imaging beneath basalt or salt. These latter applications will be discussed here.

Electromagnetic methods fall into two main categories, both of which measure the resistivity of the sub-surface. Controlled source electromagnetic (CSEM) methods use a man-made source to transmit signals through the earth to a receiver array. By studying the received signals using a combination of forward modelling and inversion, the resistivity of the sub-surface can be determined. Such methods can be applied to the sub-basalt imaging challenges both onshore (see for example Strack and Pandey 2007; Colombo et al., 2012), and offshore (see for example MacGregor and Sinha, 2000. For the purposes of illustration, here the offshore case is considered (Figure 1). Reviews of this technology are provided by Constable and Srnka (2007) and MacGregor and Tomlinson (2014) among others.

In contrast magnetotelluric (MT) methods use naturally generated electromagnetic fields as a source. Both the electric and magnetic fields from these signals are measured at the seafloor, and by analysing the transfer function between these fields as a function of signal frequency, the resistivity of the sub-surface can be constrained. These methods can also be applied to sub-basalt imaging problems both onshore (for example Warren and Srnka, 1992; Morrison et al., 1996; Withers et al., 1994; Pandey et al., 2009) and offshore (for example Jegen et al., 2009). Once again the offshore case is considered here (Figure 1).

CSEM and MT methods are complementary both in terms of acquisition (they can often be acquired simultaneously) and sensitivity. This will be illustrated using a simple synthetic example.

Sensitivity considerations

Figure 2a shows a simplified 2D structure consisting of a layer of resistivity 200 Ωm which thickens from 1km to 3 km representing a basalt flow, overlying a lower resistivity region representing a package of sub basalt sediments with resistivity 10 Ωm. These are overlain by 1km of sediments and underlain by a resistive crystalline basement. The structure is assumed to

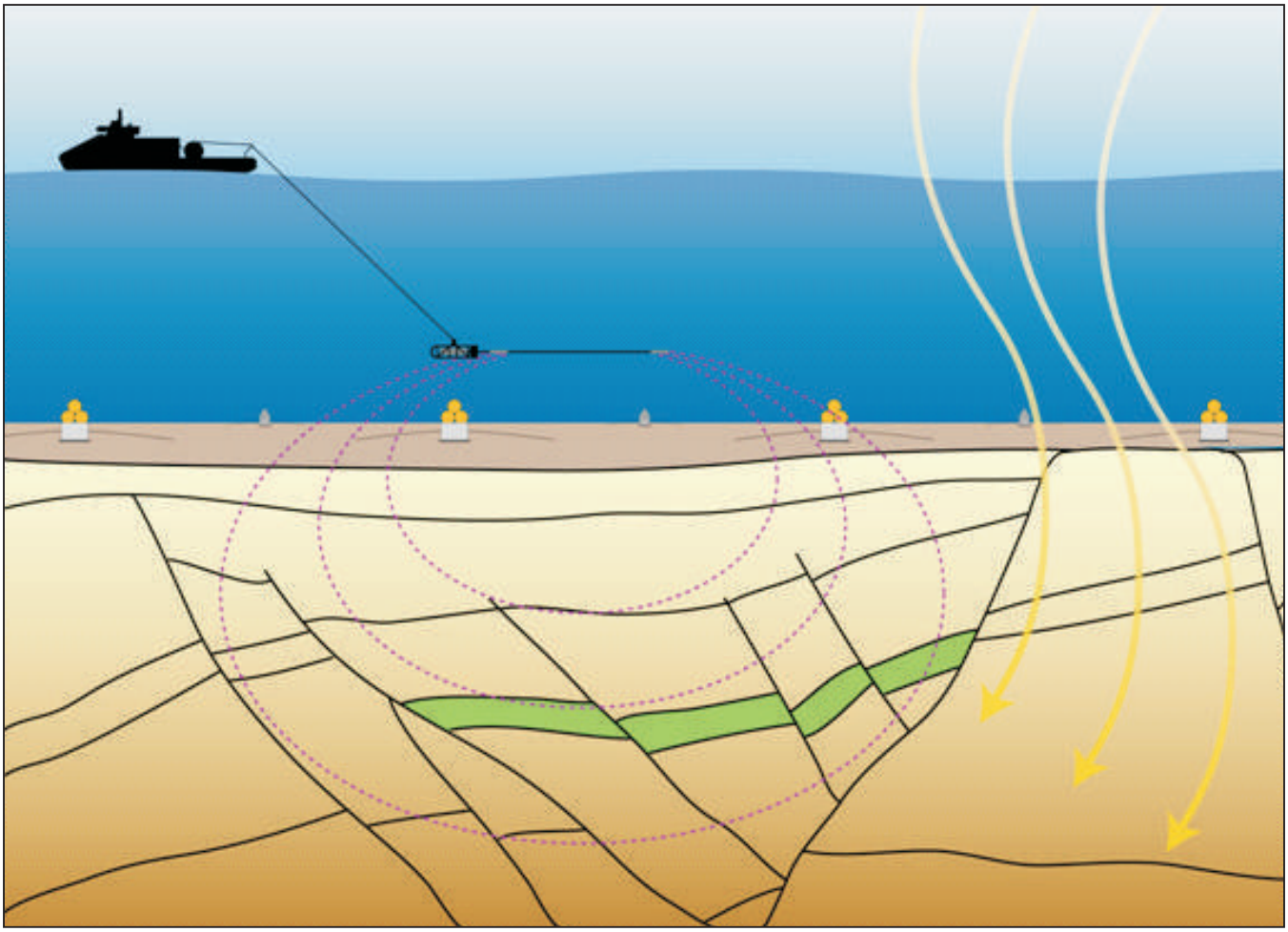

Figure 1: Electromagnetic methods offshore. CSEM uses a horizontal electric dipole source towed in the water column to transmit low frequency signal (typically a few tenths to a few tens of Hz) through the earth to an array of receivers. Analysis of the amplitude and phase of the resulting signal allows resistivity in the earth to be determined to typically 3-5 km depth below seafloor. MT methods use naturally generated electromagnetic fields as a source (yellow arrows). By studying the transfer function between measured electric and magnetic fields, resistivity can be determined to tens or hundreds of km below the seafloor, depending on the signal frequency recorded. For hydrocarbon exploration applications, signal periods of 1s-10,000 s are typical.

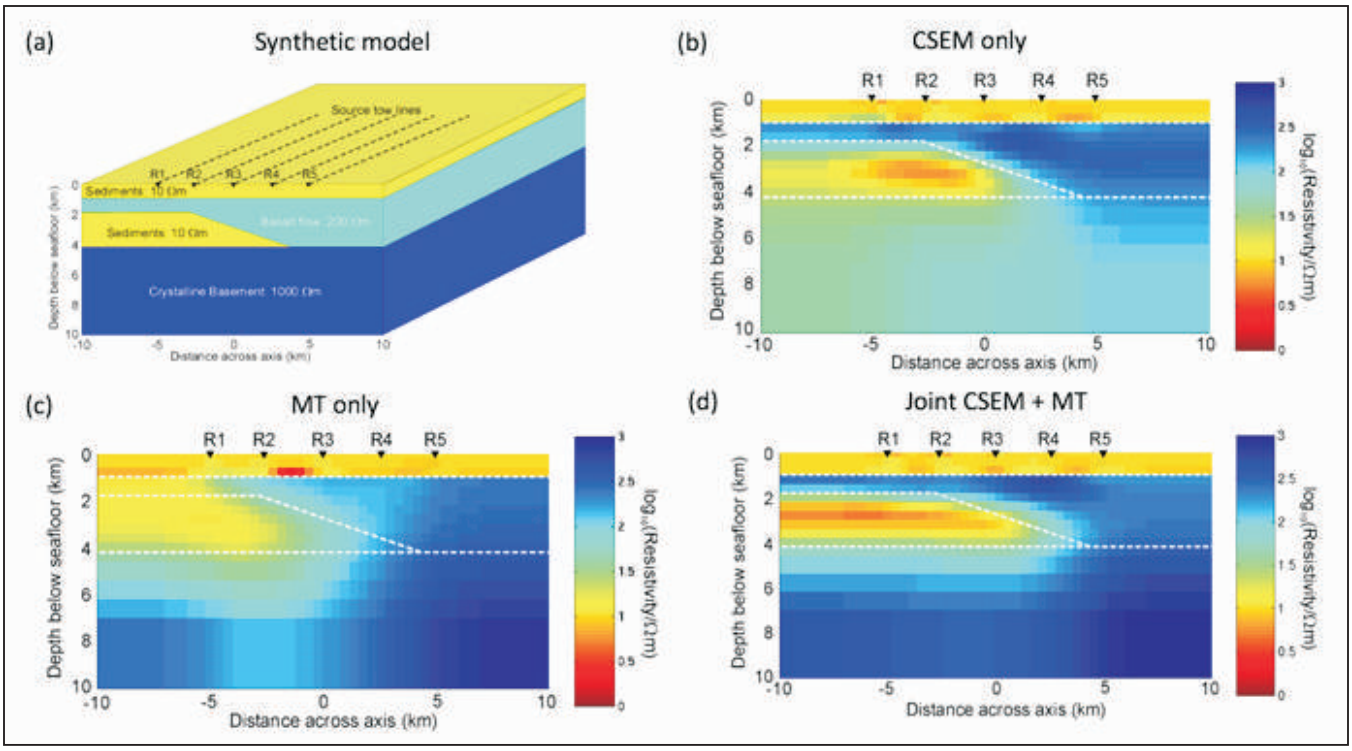

Figure 2: Simple 2D synthetic example illustrating the benefit of combining CSEM and MT data. (a) Synthetic model representing a basalt flow, sub-basalt sediments and basement. Synthetic CSEM and MT data were generated from this model, assuming five seafloor receivers (R1-R5) and five along strike source tows. (b) Inversion of the CSEM data alone. (c) Inversion of MT data alone. (d) Joint inversion of the CSEM and MT data. See text for discussion.

be isotropic in this simple example. The water depth is taken to be 1km. There are three challenges to address:

1. Can the thickness of the basalt be resolved ?
2. Can the presence and properties of the sub-basalt sediments be identified ?
3. Can the depth to basement (or the thickness of the sediments) be determined ?

To answer these questions, a synthetic CSEM and MT survey is undertaken. Five receivers are deployed on the seafloor (labelled R1 to R5 in figure 2). For the CSEM survey these record multi-azimuth data from five source tow lines towed along the invariant direction of the 2D model. The transmission frequency is 1Hz. The same five receivers also record MT data, in this case providing data at periods of 5 s to 1000 s. Both CSEM and MT data were contaminated with Gaussian noise to mimic realistic survey conditions. The synthetic data were then inverted, both separately and jointly using the Occam algorithm of Constable et al., 1987, implemented as described in MacGregor and Sinha, 2000 and extended to the joint inversion case. In all cases it is assumed that the top of the basalt can be imaged effectively using seismic data. This boundary is therefore included as a break in the smoothness constraint in the inversion. The results are shown in Figures 2b, c and d.

Looking first at the inversion of the CSEM data by itself (Figure 2b), it is clear that the resistive basalt layer is well resolved, especially where it is thin. The horizontal dipole used in the CSEM method applied in this example excites vertical current loops in the earth, making the resulting data particularly sensitive to resistive features that are thin compared to their depth of burial (MacGregor and Sinha, 2000; Constable and Srnka, 2007). The presence of the lower resistivity sub basalt sediments is also well resolved. However looking at the deeper structure, the presence of the resistive basement, and hence the thickness of the sub-basalt sedimentary sequence is not resolved. The CSEM signals do not penetrate far enough to resolve the structure at this depth.

Turning to the inversion of the MT data alone (Figure 2c), the greater depth penetration of the MT signals now allows the presence of the basement to be resolved. The sub-basalt sediments are also resolved as a low resistivity feature. However in this case the basalt is not resolved where it is at its thinnest. The MT method relies on predominantly horizontal current flow and is therefore much less sensitive to resistive structure when such structure is thin.

The joint inversion of the CSEM and MT data is shown in Figure 2c, and the benefit of combining the data types is clear. The sub-basalt structure is now well resolved. The CSEM data constrain the basalt (especially where it is thin) and the sub-basalt sediments. The MT data provide further constraint on the sub-basalt sediments, but also the basement. Taken together CSEM and MT data provide a good image of the resistivity structure.

The simple 2D example shown above assumes that the basalt is homogeneous and isotropic. In reality basalt is extremely heterogeneous, made up of stacks of individual flows interspersed by sediment, tuff and weathering layers.

This makes the basalt extremely anisotropic, and this electrical anisotropy has a significant effect on the measured electromagnetic response.

To illustrate this, Figure 3a shows a 1D model in which the basalt layer is constructed from a stack of layers of varying thickness and resistivity. The distribution of layer thicknesses is based on mapped basalt flows in eastern Iceland and layer resistivities increase with layer thickness. Layers are sampled randomly from the thickness/resistivity distribution and stacked to make the complete flow sequence to be modelled. This is representative of resistivity variations observed in basalt sequences in well log data (Pandey et al., 2008). The rapidly changing resistivity leads to a high anisotropic basalt layer. Also show in Figure 3a are the bulk harmonic average resistivity, representative of an effective horizontal resistivity (red) and the bulk arithmetic average resistivity, representative of an effective vertical resistivity (blue).

Figure 3b shows the amplitude and phase of the inline CSEM electric field. The response of the basalt flow model most closely resembles that of an isotropic model where the bulk resistivity of the basalt is the vertical resistivity of the anisotropic model. Since the bulk vertical resistivity is relatively high in this case, CSEM sensitivity to the basalt is good. In contrast the MT response shown in Figure 3c most closely resembles that of the bulk horizontal resistivity of the basalt layer. Not only is the MT response less sensitive to a resistive basalt layer in general if it is thin, heterogeneities in the basalt leading to a lower horizontal resistivity may further erode the sensitivity. It is therefore important to take such electrical anisotropy into account when analysing electromagnetic data.

Table 1 summarises the CSEM and MT sensitivity to basalt and sub-basalt structure in terms of the three questions posed at the start of this section. Joint MT-CSEM analysis has been applied in practice to the problem of sub-basalt imaging: present an excellent case study on the inversion of MT and CSEM data to constrain basalt and sub-basalt structure in the Faroe-Shetland trough, and Panzer et al., (2016) used the results of CSEM and MT data inversions to help constrain velocity model building for seismic migration.

Multi-physics integration with seismic data

Combining CSEM and MT data can provide improved images of the resistivity structure of the sub-surface. However often the goal of a geophysical exercise is to improve the seismic image. In this case CSEM and/or MT data must be combined with seismic information. When combining multiple data types, each measuring a different physical property of the earth (for example velocity and resistivity in the case of seismic and EM), it is necessary to find a relationship that couples the parameter domains (Moorkamp et al., 2010). Two methods have been formulated to

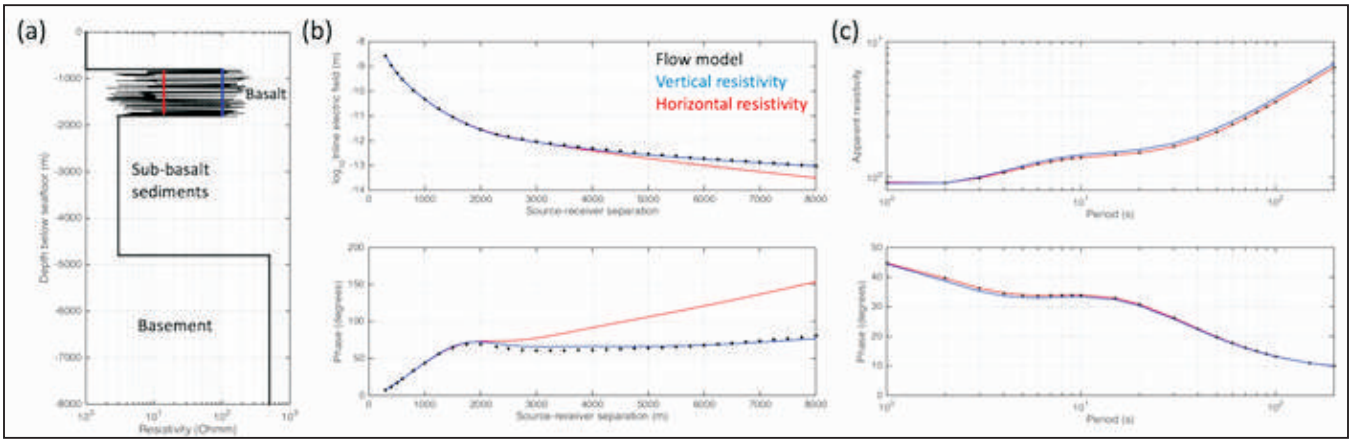

Figure 3: (a) Synthetic basalt flow model (black) in which the basalt is composed of flows of varying thickness and resistivity. This makes the resulting model extremely anisotropic. In this case the equivalent horizontal resistivity (bulk harmonic average) is 14 Ωm (red) and the equivalent vertical resistivity (bulk arithmetic average) is 102 Ωm (blue). (b) Amplitude and phase of the inline CSEM electric field. Black symbols show the response of the basalt flow model, whilst red and blue curves show the response of the equivalent horizontal and vertical resistivity models. (c) MT apparent resistivity and phase for the flow model (black symbols), equivalent horizontal (red) and vertical resistivity (blue) models.

Table 1: Summary of the relative sensitivity of CSEM and MT methods.

	MT	CSEM
Can the thickness of the basalt be resolved ?	MT has low sensitivity to resistive basalt layers unless they are thick.	CSEM is extremely sensitive to thin basalt sequences.
Can the presence and properties of the sub-basalt sediments be identified ?	MT is sensitive to the bulk properties of the sub-basalt sediments (but not details of the structure).	CSEM is sensitive to the bulk properties of the sub-basalt sediments (but not details of the structure).
Can the depth to basement (or the thickness of the sediments) be determined ?	MT is sensitive to the presence and depth of resistive basement.	CSEM will not constrain basement if the depth is greater than 3-4km.

accomplish this:

1. Coupling through rock physics relationships, in which different physical domains are linked through deterministic rock physics models, or empirical relationships derived from well log information (Jegen et al., 2009). This approach results in a strong coupling between domains, and if the functional relationship between the parameters (for example velocity and resistivity) varies over the survey area this should be taken into account. The likely variation away from well log calibration points is in general unknown, so this is often hard to do.
2. Coupling through structure, in which structural similarity between models in different domains is ensured through cross gradient constraints (Gallardo and Meju, 2004; Moorkamp et al., 2013). This is a slightly weaker constraint, where there is no explicit parameter coupling.

Here we present an example from offshore India (MacGregor et al., 2012), in which CSEM data were used to guide the construction of a velocity model to improve the seismic imaging of sediments obscured by a layer of Deccan basalt. Figure 4 outlines the workflow used for this case. Initial seismic imaging provides structural constraints in the first instance, primarily the depth to the top of the basalt layer. This is used as a constraint in the inversion of the CSEM data for an initial resistivity volume. From this, using an appropriate link between velocity and resistivity, a new velocity model can be constructed and the seismic data re-imaged. This process is repeated until a good result is achieved.

Figure 5 shows the results of this process. The initial seismic image is shown in the upper panel. Although the top basalt boundary is clear, there is little coherent seismic energy below this, and the base basalt boundary is obscured. This presented a problem when designing the marine EM campaign. If the basalt were thick, then pre-survey sensitivity analysis showed marine MT methods would be best suited to determining base basalt and sub-basalt structure. However if the basalt was thin (less than about 1km), it would be invisible to MT methods, and CSEM would be required. Given the structural uncertainty, both datasets were acquired as a contingency.

The middle panel of Figure 5 shows a resistivity section derived from CSEM analysis, co-rendered with the initial seismic image: the basalt turned out to the thin, and therefore most effectively imaged using CSEM data (note that the MT data were still useful in constraining sub-basalt and basement structure). The top basalt boundary, clearly imaged in the initial seismic result, is included in the inversion as a structural constraint, improving the resolution of the result. From this resistivity section, the base basalt boundary can be established. Modelling suggests that the point at which the vertical gradient in resistivity is maximum provides a good proxy for the boundary in this situation (MacGregor and Sinha, 2000).

Once this boundary was established a revised velocity model was constructed and through a series of iterative steps the final image in the lower panel of Figure 5 was obtained. Comparing the top and bottom seismic images in Figure 5, it is clear that the integration of marine EM derived resistivity information has dramatically improved the quality of the seismic image in the sub-basalt area.

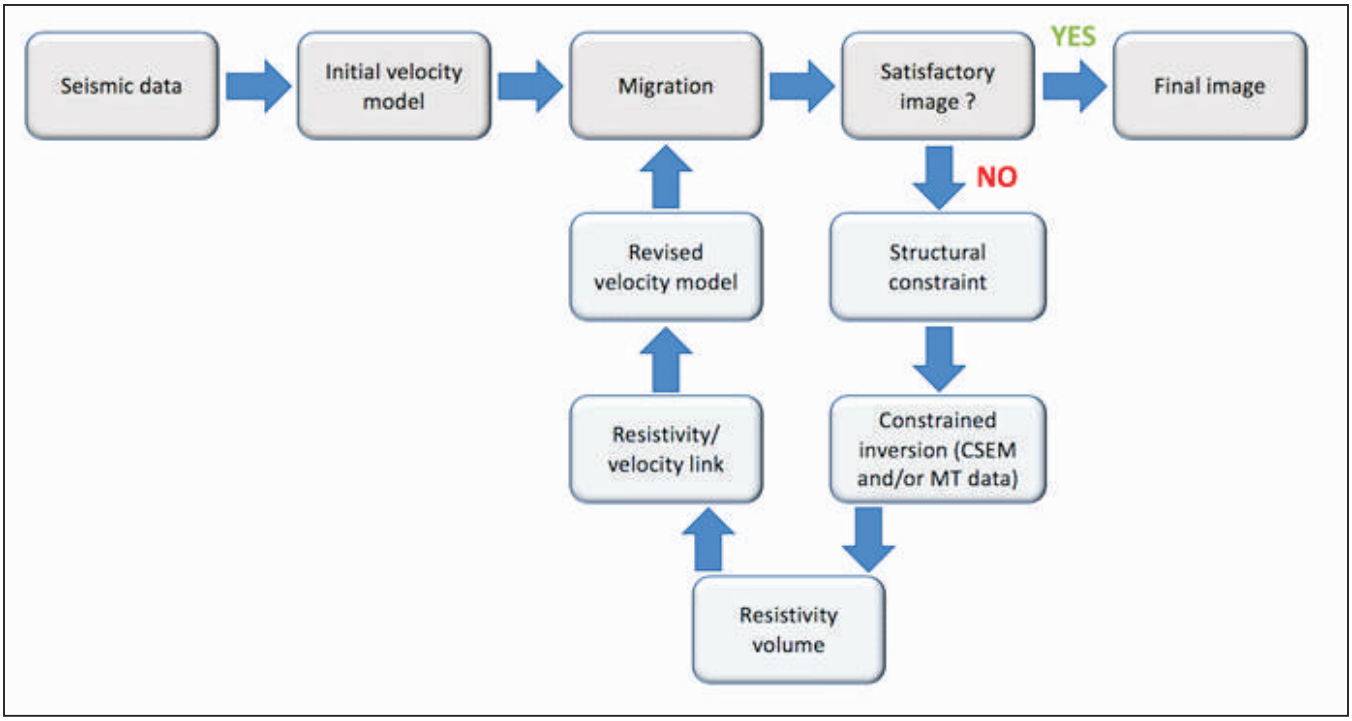

Figure 4: Workflow applied in the example presented here. The top row, shaded grey, represents a standard seismic imaging workflow. Adding the multi-physics loops, shaded blue, can dramatically improve the seismic image that is obtained.

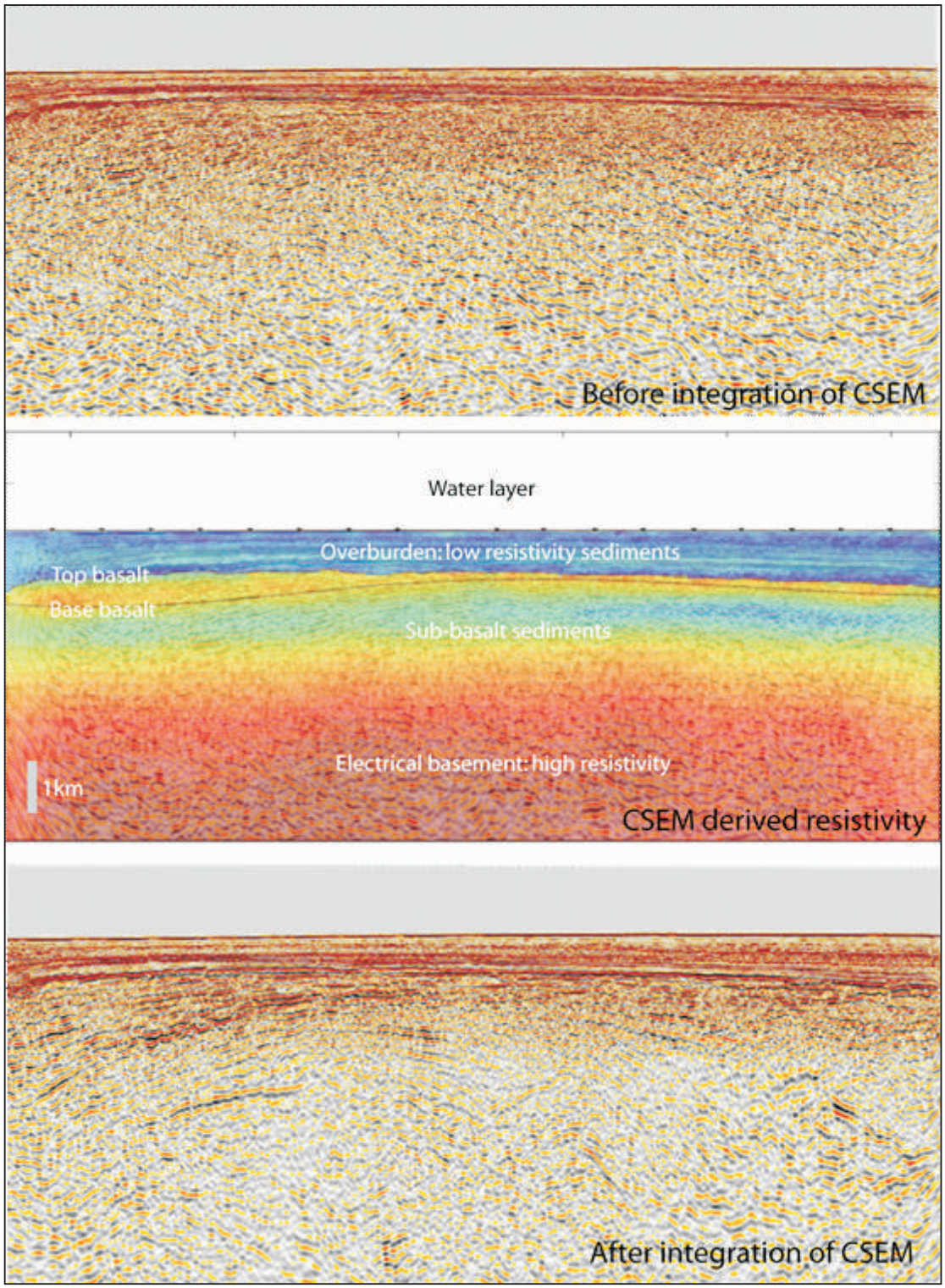

Figure 5: Example of improved seismic imaging sub-basalt by integrating seismic and CSEM workflows. Upper panel: Initial seismic image. Little can be discerned beneath the top basalt boundary. Middle panel: CSEM derived resistivity co-rendered with the initial seismic image. Yellow-red colours indicate high resistivity. The basalt layer is in this case relatively thin (less than 1km). The thin black line delineates a base basalt boundary picked from the resistivity data. Lower panel: Final seismic image after incorporation of EM-derived information on basalt thickness into the velocity model. Sub-basalt structure is now much more successfully imaged.

The approach presented here is similar to that of Panzer et al., 2016, and has the advantage that it can be undertaken using widely available tools and algorithms without the need for specialist technology. Intermediate results can also provide insight into the problem, and the workflow can be updated if necessary. This process can of course be encapsulated within a joint inversion algorithm, and excellent results have been obtained both for the sub-basalt and the related sub-salt

imaging problems (see for example Colombo et al., 2007; Jegen et al., 2009; Medina et al., 2012; Moorkamp et al., 2013; Colombo et al., 2018).

Conclusions

Key to success in multi-physics workflows that combine seismic with CSEM, MT or other measurements is ensuring that the best tool or combination of tools to address the question of interest is applied. This requires careful sensitivity analysis for both seismic and non-seismic methods to be carried out before a survey is contemplated or acquired. However if this is done, in areas of challenging geology, a multi-physics approach can significantly improve the resolution of sub-surface structure.

Acknowledgements

The example shown in this paper was initially presented by MacGregor et al., at the 1st EAGE workshop on EM in the hydrocarbon industry, Singapore, April 2012. The author would like to thank Reliance for permission to show this example.

References

Alvarez, P., Marcy, F., Vrijlandt, M., Skinnemoen, O., MacGregor, L., Nichols, K., Keirstead, R., Bolivar, F., Bouchrara, S., Smith, M., Tseng, H-W and Rappke, J., 2018, Multi-physics characterisation of reservoir prospects in the Hoop area of the Barents Sea, *Interpretation, **6 (3)**, SG1-SG17.*

Alvarez, P., Alvarez, A., MacGregor, L., Bolivar, F., Keirstead, R. and Martin, T., 2017, Reservoir property prediction using CSEM, pre-stack seismic and well log data: Case study in the Hoop Area, Barents Sea, Norway, 2017, *Interpretation, **5**, SE43-SE60*

Colombo, D., Rovetta, D., and Turkoglu, E., 2018, CSEM regularised seismic velocity inversion: a multiscale, hierarchical workflow for sub-salt imaging. *Geophysics, **83**, B241-B252*

Colombo, D., Keho, T., and McNeice, G., 2012, Inetgrated seismic-EM workflow for sub-basalt exploration in northwest Saudi-Aribia. *The Leading Edge, January 2012*

Colombo, D. and Stefano, M. D., 2007, Geophysical modeling via simultaneous joint inversion of seismic, gravity, and electromagnetic data: application to prestack depth imaging, *Leading Edge,* **26**(3), 326–331.

Constable, S., and Srnka, L., 2007, An introduction to marine controlled source electromagnetic methods for hydrocarbon exploration, *Geophysics, **72**, WA3-WA12*

Gallardo, L. A., and M. A., Meju, 2004, Joint two-dimensional DC resistivity and seismic travel time inversion with cross-gradients constraints, J. Geophys. Res., 109, B03311

Heinke, B., Moorkamp, M., Jegen, M., Hobbs, R. W., and Berndt, C., 2014, 2D and 3D joint inversion of seismic, MT and gravity data from the Faroe Shetland Basin, *EAGE Annual meeting 2014, Expanded Abstract.*

Jegen, M. D., Hobbs, R. W., Tarits, P., and Chave, A., 2009, Joint inversion of marine magnetotelluric and gravity data incorporating seismic constraints. Preliminary results of sub-basalt imaging off the Faroe Shelf: *Earth and Planetary Science Letters, **282,** no. 1-4, 47–55.*

MacGregor, L. M., and Tomlinson, J., 2014, Marine controlled source electromagnetic methods in the hydrocarbon industry: A tutorial on method and practice. *Interpretation, **2**, SH13-SH32*

MacGregor, L. M., 2012a, Integrating seismic, CSEM and well log data for characterisation of reservoirs, *EAGE workshop on EM in hydrocarbon exploration, April 2012, Singapore.*

MacGregor, L. M., 2012b, Integrating seismic, CSEM and well log data for reservoir characterisation, *The Leading Edge, 268-277.*

MacGregor, L. M., and Sinha M. C., 2000, Use of marine controlled source electromagnetic sounding for sub-basalt exploration. *Geophysical Prospecting*, **48**, 1091-1106.

Medina, E. A., Lovatini, F. G., Andreasi, S. Re, and Snyder, F., 2012, Simul-taneous joint inversion of 3D seismic and magnetotelluric data from the walker ridge: First Break, 30, 85–88.

Moorkamp, M., Heincke, H., Jegen, M., Roberts, A. W., and Hobbs, R. W., 2010, A framework for 3D joint inversion of MT, gravity and seismic refraction data: *Geophysical Journal International*, **184**, 477–493.

Moorkamp, M., Roberts, A. W., Jegen, M., Heincke, B., and Hobbs, R. W., 2013, Verification of velocity-resistivity relationships derived from structural joint inversion with borehole data, *Geophys. Res. Lett.,* **40**, *1-6*

Morrison H. F., Shoham Y., Hoversten G. M., and Torres-Verdin C. 1996, Electromagnetic mapping of electrical conductivity beneath the Columbia basalts. *Geophysical Prospecting* **44**, 963–986.

Pandey, D., Singh, Sinha, M., and MacGregor, L., 2009, Structural imaging of Mesozoic sediments of Kachchh, India, and their hydrocarbon prospects, *Marine and Petroleum Geology, **27**, 1043-1050*

Pandey, D., MacGregor, L., Sinha, M., and Singh S., 2008, Feasibility of using magnetotelluric for sub-basalt imaging at Kutch, India, *Applied Geophysics, **5**, number 1*

Panzer, M., Morten, J. P., Weibull, W. W., and Arnsten, B., 2016, Integrated seismic and EM model building applied to improve sub-basalt depth imaging in the Faroe-Shetland basin, *Geophysics, **81**, E57-E68.*

Smallwood, J., White, R. S., and Staples, R., 1998, Deep crustal reflectors under Reydarfjordur, eastern Iceland: crustal accretion above the Iceland mantle plume. *Geophys. J. Int., **134**, 277-290.*

Strack K. M., and Pandey P. B., 2007, Exploration with controlled-source electromagnetic under basalt cover in India. *The Leading Edge* **26**, 260–363.

Warren R. K., and Srnka L.J., 1992, Exploration in the basalt- covered areas of the Columbia River Basin, Washington, using electromagnetic array profiling (EMAP). *Geophysics* **57**, 986– 993.

Withers R., Eggers D., Fox T., and Crebs T. 1994, A case study of integrated hydrocarbon exploration through basalt. *Geophysics* **59**, 666–1679.